

# A New Ultra-dense Group of Obscured Emission-Line Galaxies

R. Weinberger and S. Tempurin

Institut für Astronomie, Leopold-Franzens-Universität Innsbruck, Technikerstrasse 25,  
A-6020 Innsbruck, Austria; ronald.weinberger@uibk.ac.at, giovanna.tempurin@uibk.ac.at

and

F. Kerber

Space Telescope - European Coordinating Facility, ESO, Karl-Schwarzschild-Strasse 2,  
D-85748 Garching, Germany; fkerber@eso.org

Received \_\_\_\_\_; accepted \_\_\_\_\_

## ABSTRACT

We present the discovery of an isolated compact group of galaxies that is extremely dense (median projected galaxy separation: 6.9 kpc), has a very low velocity dispersion ( $\sigma_{2D} = 67 \text{ km s}^{-1}$ ), and where all observed members show emission lines and are morphologically disturbed. These properties, together with the lack of spirals and the presence of a prominent tidal tail make this group one of the most evolved compact groups.

*Subject headings:* galaxies: compact — galaxies: interactions — galaxies: starburst — galaxies: evolution

## 1. Introduction

Recent works support the hierarchical galaxy formation theory, in which massive galaxies form by subsequent mergers of smaller systems (Larson 1990; Rauch, Haehnelt, & Steinmetz 1997). In the context of understanding the formation and evolution of galaxies, compact groups (CGs) play an eminent role and can be regarded as a unique laboratory for the study of galaxy interactions, tidally triggered starburst or active galactic nuclei (AGN) activity, and the merging of galaxies.

CGs combine low velocity dispersions (compared to galaxy clusters), small size and high spatial density. This combination suggests that interactions and mergers should occur frequently in these groups. Details of these processes are, however, under lively discussion and, particularly, the latest stages of the evolution of CGs are widely unknown. The reason is that known high-density CGs are scarce; however, there are examples like parts of HCG 94 (Pildis 1995) and of HCG 95 (Iglesias-Páramo & Vílchez 1998; Rodrigue et al. 1995).

As to remnants of CGs, results are even more meager: only two fossil CGs have been found and the coalescence processes that lead to the expected bright field ellipticals appear to proceed much slower than anticipated (Ponman 1995; Mulchaey & Zabludoff 1999). For our understanding of the processes it is important to find and study at least one CG that shows, as a whole, characteristics of a very advanced phase of evolution. Our observations indicate that we have found the most promising candidate yet. It was recognized by us as a morphologically unusual object (Weinberger 1995) and will be called CG1720-67.8.

## 2. Observations and Data Reduction

For the study in this paper we used both imaging and spectroscopic data. A 900 sec V frame (centered at  $\lambda 5610 \text{ \AA}$ ; seeing 1.8 arcsec) was obtained at the Du Pont 2.5m-telescope

of Las Campanas Observatory, equipped with a  $2048^2$  pixel<sup>2</sup> Tek5 CCD having a pixel-size of  $24\ \mu\text{m}$  and giving a resolution of  $0.259\ \text{arcsec/pixel}$  in an  $8' \times 8'$  field of view. The frame was processed by means of the Potsdam Image Processing System. This package includes both a standard reduction procedure and a laplacian adaptive filtering procedure. This adaptive filtering method, developed to suppress the background noise and to distinctly enhance faint structures hidden in strong long-scale luminosity variations (Richter et al. 1991; Lorenz et al. 1993), allows to put in evidence details of extended objects as well as faint objects otherwise not clearly visible on an image.

Two long-slit spectra (1800 sec and 1500 sec), taken under good seeing conditions ( $< 1''$  in the second case) were obtained in May 1997 at the MPI 2.2m telescope in La Silla, and in February 1998 at the Du Pont 2.5m telescope of Las Campanas Observatory, respectively. For the former spectrum we had a spatial resolution of  $0.26\ \text{arcsec/pixel}$  and a dispersion of  $2\ \text{\AA/pixel}$  over the range  $3850 - 8000\ \text{\AA}$ ; the spectral resolution was  $\sim 12\ \text{\AA}$ . For the latter spectrum the spatial resolution was  $0.56\ \text{arcsec/pixel}$  and the dispersion  $2\text{\AA/pixel}$  over the range  $3770 - 7180\text{\AA}$ ; the spectral resolution was  $\sim 4\ \text{\AA}$ . The standard stars LTT 7379 and CD -32d9927 were used to perform the flux calibration.

The standard reduction steps (mean bias subtraction, flat field correction, wavelength calibration, and atmospheric extinction correction) as well as line flux and position measurements were carried out by means of the IRAF packages. The spectra of all the galaxies of the group show emission lines and, in two cases, pronounced absorption lines too. Emission line fluxes were measured after a template spectrum of the underlying stellar component, obtained from a composition of elliptical galaxy spectra and conveniently diluted to best fit the absorption features, had been subtracted from the spectra, following Ho, Filippenko, & Sargent (1993). Particular care was taken to uncover the  $\text{H}\beta$  emission line, which is embedded in the corresponding Balmer absorption line feature. A further

correction was applied to eliminate the telluric atmospheric absorption bands falling at the wavelength of  $H\alpha$ .

### 3. The Images

In Figure 1, we present the CCD  $V$  frame: the image as reduced in the standard way is shown in Figure 1a, its filtered counterpart, displayed with contour lines and with spectral slit positions superposed (see below) is presented in 1b and as a color image in Figure 1c.

A wealth of details is visible: the brightest object is an elliptical galaxy (no. 2); the next brightest galaxy (no. 4) also appears to be of elliptical type in Figure 1a, but shows a more complicated structure in Figure 1b and 1c, where one notices an elongated (double?) nucleus and outer contours that are reminiscent of two (disk) galaxies that have almost merged. No. 1, the third-brightest galaxy is disturbed by no. 2, looks elliptical-like (Figure 1a), but shows some internal structure in Figure 1c. Most spectacular is the arc: at both ends there are distinct brightness enhancements; the northern one (the fourth-brightest object) is numbered 3, and the other 7. No. 5, half-way between no. 4 and a star, either is the end of a tail connected to no. 4 (see Figure 1c) or is an individual object. A faint diffuse extended object is seen south-west of the star just mentioned, close to the western rim of Figure 1c. Finally, number 6 was assigned to a location where one slit position crossed the arc. CG1720-67.8 is very isolated: there is no obvious other galaxy within 11 times the diameter (ca.  $30''$ ) of this ensemble of galaxies; the next cataloged galaxy is about  $1^\circ$  away. The group shows a strikingly high degree of interactions between its member candidates.

Although the  $V$  frame was uncalibrated, comparison with the images on the SERC J and ESO R film copies allowed an estimate of the  $V$ -magnitudes of the brightest member candidates ( $\pm \sim 0.5$  mag): we estimate that the objects range from 17.5 (no. 2), to 20.5

(no. 3). That is, the four brightest member candidates are within 3 mag, and the group is compact and isolated - it thus fulfills the criteria of Hickson (1982) compact groups.

#### 4. The Spectra

We found emission lines in all the objects (nos. 1 - 6) of CG1720-67.8 covered by the slits and absorption lines in nos. 2, 4, 5, and 6. The spectra are available on astro.uibk.ac.at (anonymous ftp) in the directory /pub/weinberger/. The emission line fluxes for the four brightest galaxies are listed in Table 1; objects nos. 5 and 6 showed  $H_\alpha$  and [N II] 6583 only.

Heliocentric radial velocities were determined from the emission lines; they are in accord with the otherwise less accurate velocities derived from absorption lines. The calibration error, estimated from the mean deviation of the measured sky line positions from the predicted ones is  $\sim 14 \text{ km s}^{-1}$  for the spectrum taken at Las Campanas and  $\sim 30 \text{ km s}^{-1}$  for the one taken at ESO. Radial velocities derived from different lines were averaged using  $1/\delta_v^2$  as weighting factor, where  $\delta_v$  is the velocity error expressed as a function of the S/N of the relevant emission-line. The variation of  $\delta_v$  as a function of S/N was derived using night-sky emission lines following the procedure described in Corsini et al. (1999). The thus calculated radial velocities, after application of the heliocentric correction and the associated errors are listed in Table 1. Hence, the mean redshift of CG1720-67.8 is  $z = 0.045$  - and the distance of the group is 179.9 Mpc (with  $H_0 = 75 \text{ km s}^{-1} \text{ Mpc}^{-1}$ , used throughout this paper).

#### 5. Discussion

### 5.1. The Star Formation Activity

In order to attempt a classification of these emission-line galaxies, we made use of diagnostic diagrams (Veilleux & Osterbrock 1987). They are shown in Figure 2. Usually, the  $[\text{N II}]/\text{H}_\alpha$  vs.  $[\text{O III}]/\text{H}_\beta$  diagram (Figure 2b) is considered to be most meaningful. We can thus infer from Figure 2 that all the galaxies under examination, with the possible exception of no. 2, undergo star formation.

We interpret this result as an indication of enhanced star formation possibly induced from tidal interactions: from studies of N-body simulations of galaxy encounters it is known that interactions drive large gas flows towards the center of galaxies, triggering massive nuclear star formation (e.g. Barnes & Hernquist 1991, Mihos & Hernquist 1996).

We carried out photoionization model calculations by means of CLOUDY90 (Ferland 1996) and found the following logarithmic values of the electron density  $n_e$  and the ionization parameter  $U$ : 2.0, –2.8; 2.0, –3.5; 2.2, –3.0; and 2.1, –3.7 for the galaxies nos. 1-4, respectively. In all four cases a non-LTE Mihalas stellar continuum with  $T = 42\,000$  K was assumed (Mihalas 1972). As we could not properly fit the observed emission line ratios assuming solar abundances for objects nos. 2 and 4, we tried to vary the nitrogen (N) and sulfur (S) abundances. A best fit to the data was obtained assuming an N abundance of 0.5 (solar units) for no. 2, and both N and S abundances of 0.5 for no. 4. Some deviations of  $[\text{O I}]/\text{H}_\alpha$  and  $[\text{S II}]/\text{H}_\alpha$  line ratios from typical H II galaxies suggest that photoionization is not the only ionization mechanism acting in these galaxies; a possible interpretation would be the presence of shocks generated from stellar winds as a consequence of bursts of star formation (Dopita & Sutherland 1995). Better spectroscopic data are needed to firmly establish the nature of the ionization mechanism.

To obtain an estimate of the star formation rates (SFRs) in the four most luminous objects, the  $\text{H}_\alpha$  luminosity has been calculated from  $\text{H}_\alpha$  fluxes using the radial velocities

listed in Table 1. According to Hunter & Gallagher (1986),  $\text{SFR} = 7.07 \cdot 10^{-42} L(\text{H}_\alpha) \text{ M}_\odot \text{ yr}^{-1}$ , taking into account all stars from 0.1 to 100  $\text{M}_\odot$  and providing a measure of the current SFR.

As the luminosity calculated refers to only to the portion of the galaxies sampled by the long-slit spectra, the SFR values have been divided by the corresponding areas occupied by the single galaxies in the slit (not taking into account the effects of seeing). Anyway, it should be considered that if the SF processes are concentrated in restricted regions of a galaxy, the SFR per unit area declines with the size of the sampled region.

We found values (Table 2) up to one order of magnitude greater than those for interacting spirals (Bushouse 1987). This means that all four galaxies are experiencing a clear enhancement of star formation.

An estimate of the number of ionizing photons required to produce the observed  $L(\text{H}_\alpha)$  is given by  $Q_{\text{ion}} = 7.3 \cdot 10^{51} (L(\text{H}_\alpha)/10^{40} \text{ erg s}^{-1})$ . This quantity can be expressed in equivalents of the number of O5 stars,  $N(\text{O5})$ , assuming that each O5 star emits  $\sim 5 \cdot 10^{49}$  ionizing photons per sec (Osterbrock 1989). The values obtained by us (Table 2) are comparable to or even higher than those found in “giant” or “supergiant” extragalactic H II regions, whose  $L(\text{H}_\alpha)$  are in the range  $10^{39} - 10^{41} \text{ erg s}^{-1}$  (Kennicutt Jr, Edgar, & Hodge 1989).

## 5.2. Comparison with Hickson Compact Groups

HCGs prove to be of great significance for the understanding of interactions between galaxies and appear to be of key interest for studying the formation of new, bright field ellipticals. Our data allow, e.g., the determination of two very important parameters to characterize CGs, namely the median projected galaxy separation (MPS) and the velocity



dispersion ( $\sigma$ ): from our four brightest galaxies we found an MPS of 6.9 kpc, much lower than 9.1 kpc for Seyferts Sextett (HCG 79), which is reported to be the most compact group (Hickson 1993), and velocity dispersions  $\sigma_{2D} = 67 \text{ km s}^{-1}$ , and  $\sigma_{3D} = 99 \text{ km s}^{-1}$ . Median values for the HCGs are MPS = 52 kpc,  $\sigma_{2D} = 200 \text{ km s}^{-1}$  and  $\sigma_{3D} = 331 \text{ km s}^{-1}$  (Hickson et al. 1992). The comparison thus convincingly shows that CG1720-67.8 is extreme with respect to these quantities.

The fact that we found activity in all our hitherto observed member galaxies is, even if taken alone, remarkable and reminds of HCG 16 (Mendes de Oliveira et al. 1998). Such a wide-spread activity underlines the prevalence of interaction and merger processes in CG1720-67.8. In addition, the prominent tail - obviously a tidal tail - that dominates the optical appearance of CG1720-67.8, is a further proof of the ongoing interaction in this group.

### 5.3. The Dust Puzzle

From  $H_\alpha/H_\beta$ , after carefully having taken hydrogen absorption features into account, we found visual extinctions ( $A_V = 3.1E_{B-V}$ ), that are variable across the field and are partly astonishingly high: we found  $A_V$  values of  $0.8 \pm 0.1$ ,  $1.6 \pm 1.2$ ,  $3.2 \pm 1.4$ , and  $2.0 \pm 0.4$  mag for objects 1 - 4, respectively. The Galactic foreground extinction is small: the remote ( $>7$  kpc) globular cluster NGC 6362 ( $\ell = 325.3^\circ$ ,  $b = -17.6^\circ$ ), only about  $1.3^\circ$  away from CG1720-67.8, has a color excess  $E_{B-V} = 0.11$  only (Zinn 1985). Provided that the derived extinctions represent the foreground obscuration of the respective galaxies, estimates of the absolute magnitudes of these galaxies are possible and the combined brightness of all these four galaxies (together with a rough estimate of the remaining objects) results in a total absolute magnitude of not more than  $-21.5$  mag for CG1720-67.8. Strangely enough, there is no counterpart in the IRAS catalogs but a very vague hint for  $60\mu\text{m}$  emission in IRAS

maps (by the way, CG1720-67.8 also has no counterpart in radio or X-ray catalogs).

Why does the plenty of dust, which is responsible for the pronounced extinction, not emit in the IRAS bands? We suggest, that it might be very cool dust that mainly radiates beyond  $100\mu\text{m}$ . If true, this may be due to dust in the group's halo, perhaps blown off by strong galactic winds.

From all pieces of evidence, taken together, we conclude that CG1720-67.8 is in all probability a group of galaxies on the verge of coalescence. If we assume that the group will evolve into an elliptical galaxy, as is generally believed for compact groups (Mulchaey & Zabludoff 1999), the end-product may hardly be a very bright field elliptical galaxy, but rather a moderately bright one. This ultra-dense compact group deserves thorough future studies - and objects of the same highly evolved species.

We are grateful to Prof. Richter, Potsdam, for making available to us the Potsdam Image Processing System.

| Line                  | Object 1                      | Object 2                        | Object 3                       | Object 4                      |
|-----------------------|-------------------------------|---------------------------------|--------------------------------|-------------------------------|
| [OII] $\lambda$ 3727  | $1.79 \pm 0.29$ ; <b>2.28</b> | $2.02 \pm 1.43$ ; <b>3.28</b>   | ...                            | ...                           |
| H $\delta$            | $0.42 \pm 0.14$ ; <b>0.49</b> | ...                             | ...                            | ...                           |
| [OIII] $\lambda$ 4959 | $0.63 \pm 0.04$ ; <b>0.62</b> | $0.27 \pm 0.21$ ; <b>0.26</b>   | $0.98 \pm 0.95$ ; <b>0.92</b>  | $0.07 \pm 0.06$ ; <b>0.07</b> |
| [OIII] $\lambda$ 5007 | $1.89 \pm 0.08$ ; <b>1.84</b> | $0.53 \pm 0.33$ ; <b>0.50</b>   | $1.81 \pm 1.07$ ; <b>1.62</b>  | $0.25 \pm 0.12$ ; <b>0.23</b> |
| HeI $\lambda$ 5876    | ...                           | ...                             | ...                            | $0.16 \pm 0.08$ ; <b>0.10</b> |
| [OI] $\lambda$ 6300   | $0.09 \pm 0.03$ ; <b>0.07</b> | $1.07 \pm 0.61$ ; <b>0.64</b>   | ...                            | $0.18 \pm 0.06$ ; <b>0.10</b> |
| [NII] $\lambda$ 6548  | $0.33 \pm 0.06$ ; <b>0.25</b> | $0.36 \pm 0.38$ ; <b>0.20</b>   | $0.96 \pm 1.07$ ; <b>0.31</b>  | $0.49 \pm 0.20$ ; <b>0.24</b> |
| H $\alpha$            | $3.80 \pm 0.15$ ; <b>2.85</b> | $5.09 \pm 2.14$ ; <b>2.85</b>   | $8.78 \pm 4.21$ ; <b>2.85</b>  | $5.76 \pm 0.86$ ; <b>2.85</b> |
| [NII] $\lambda$ 6583  | $0.67 \pm 0.06$ ; <b>0.50</b> | $1.09 \pm 0.69$ ; <b>0.61</b>   | $3.07 \pm 1.87$ ; <b>0.99</b>  | $1.86 \pm 0.35$ ; <b>0.91</b> |
| [SII] $\lambda$ 6716  | $0.44 \pm 0.07$ ; <b>0.32</b> | $1.64 \pm 1.13$ ; <b>0.88</b>   | $3.63 \pm 3.16$ ; <b>1.09</b>  | $1.00 \pm 0.28$ ; <b>0.47</b> |
| [SII] $\lambda$ 6731  | $0.35 \pm 0.06$ ; <b>0.26</b> | $1.05 \pm 0.74$ ; <b>0.56</b>   | $1.54 \pm 2.51$ ; <b>0.46</b>  | $0.73 \pm 0.22$ ; <b>0.34</b> |
| F(H $\beta$ )         | $67.2 \pm 2.0$ ; <b>16.06</b> | $14.36 \pm 5.03$ ; <b>83.22</b> | $4.32 \pm 1.81$ ; <b>130.5</b> | $16.3 \pm 2.1$ ; <b>13.74</b> |
| $V_{\text{hel}}$      | $13430 \pm 1$                 | $13558 \pm 4$                   | $13523 \pm 4$                  | $13427 \pm 10$                |

Table 1: Emission line fluxes, in units of H $\beta$ ; bold numbers are extinction corrected intensities. F(H $\beta$ ) is in units of  $10^{-16}$  erg s $^{-1}$  cm $^{-2}$ . Heliocentric radial velocities are given in the last line; for objects no. 5 and 6 they are  $13547 \pm 45$  and  $13639 \pm 88$  km sec $^{-1}$ , respectively.

| (1)   | (2)                 | (3)   | (4)    | (5)   | (6)              | (7)            |
|-------|---------------------|-------|--------|-------|------------------|----------------|
| Id.   | $L(\text{H}\alpha)$ | $SFR$ | $Area$ | $SFR$ | $Q_{\text{ion}}$ | $N(\text{O5})$ |
| <hr/> |                     |       |        |       |                  |                |
| 1     | 17.6                | 1.24  | 8.26   | 15.0  | 12.8             | 2560           |
| 2     | 9.30                | 0.66  | 9.06   | 7.3   | 6.79             | 1358           |
| 3     | 1.45                | 0.1   | 8.38   | 1.2   | 1.06             | 212            |
| 4     | 15.0                | 1.06  | 10.7   | 9.9   | 10.9             | 2190           |

Table 2:  $L(\text{H}\alpha)$  and star formation rates. Data are given in the following units: col. (2)  $10^{40}$  erg s $^{-1}$ , (3)  $\text{M}_{\odot}$  yr $^{-1}$ , (4)  $10^6$  pc $^2$ , (5)  $10^{-8}$   $\text{M}_{\odot}$  yr $^{-1}$  pc $^{-2}$ , (6)  $10^{52}$  phot s $^{-1}$ , and col. (7) number of O stars.

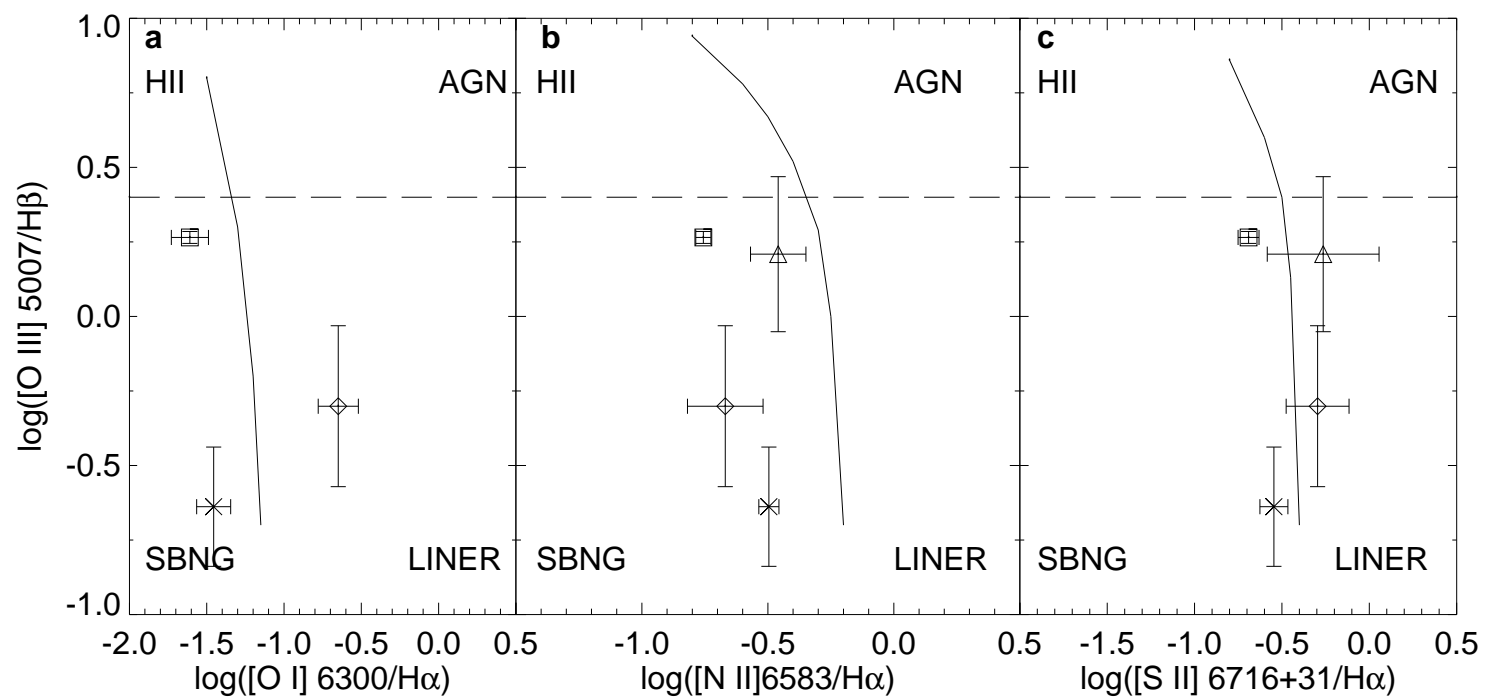
## REFERENCES

- Barnes, J. E., & Hernquist, L. 1991, ApJ, 370, L65
- Bushouse, H. A. 1987, ApJ, 320, 49
- Corsini, E. M., et al. 1999, A&A, 342, 671 A
- Coziol, R. 1996, A&A, 309, 345
- Coziol, R., Ribeiro, A. L. B., de Carvalho, R. R., & Capelato, H. V. 1998, ApJ, 493, 563
- Dopita, M. A., & Sutherland, R. S. 1995, ApJ, 455, 468
- Ferland, G. 1996, Hazy, a Brief Introduction to CLOUDY, Univ. of Kentucky, Dept. of Physics & Astronomy, int. report
- Hickson, P. 1982, ApJ, 255, 382
- Hickson, P. 1993, Astrophys. Lett.& Comm., 29, 1
- Hickson, P., Mendes de Oliveira, C., Huchra, J. P., & Palumbo, G. C. 1992, ApJ, 399, 353
- Ho, L. C., Filippenko, A. V., & Sargent, W. L. W. 1993, ApJ, 417, 63
- Hunter, D. A., & Gallagher III, J. S. 1986, PASP, 98, 5
- Iglesias-Páramo, J., & Vílchez, J. M. 1998, AJ, 115, 1791
- Kennicutt Jr, R. C., Edgar, B. K., & Hodge, P. W. 1989, ApJ, 337, 761
- Larson, R. B. 1990, PASP, 102, 709
- Lorenz, H., Richter, G. M., Capaccioli, M., & Longo, G. 1993, A&A, 277, 321
- Mendes de Oliveira, C., Plana, H., Amram, P., Bolte, M., Boulesteix, J. 1998, ApJ, 507, 691

- Mihalas, D. 1972, *Non-LTE Model Atmospheres for B and O Stars*, Boulder: NCAR
- Mihos, J. C., & Hernquist, L. 1996, *ApJ*, 464, 641
- Mulchaey, J. S., & Zabludoff, A. I. 1999, *ApJ*, 514, 133
- Osterbrock, D. E. 1989, *Astrophysics of Gaseous Nebulae and Active Galactic Nuclei*, University Science Books, Mill Valley, CA
- Pildis, R. A. 1995, *ApJ*, 455, 492
- Ponman, T. J. 1995, *Nature*, 369, 462
- Rauch, M., Haehnelt, M. G., and Steinmetz, M. 1997, *ApJ*, 481, 601
- Richter, G. M., Lorenz, H., Böhm, P., & Priebe, A. 1991, *Astron. Nachr.*, 312, 345
- Rodrigue, M., et al. 1995, *AJ*, 109, 2362
- Veilleux, S., & Osterbrock, D. E. 1987, *ApJS*, 63, 295
- Weinberger, R. 1995, *PASP*, 107, 58
- Zinn, R. 1985, *ApJ*, 293, 424

Fig. 1.— Images of the new compact group CG1720-67.8. North is up and east is to the left. - (a) A 15 min exposure in V (centered at 5610 Å). (b) The observed V frame processed by means of the Potsdam Image Processing System, displayed in the form of brightness contours. Spectroscopic slit positions and widths are shown too, where the segments give the assignment of the spectral emission to the different objects. The member galaxies plus some brightness enhancements are numbered (see text). The unnumbered roundish objects (north-west of no. 5, northeast of no. 7, and close to the left rim of 1b) are foreground stars. Galaxy no. 2 ( $\alpha = 17^{\text{h}}20^{\text{m}}28.8^{\text{s}}$ ,  $\delta = -67^{\circ}46'25.2''$ ; J2000) serves as the origin for relative equatorial coordinates c) The processed frame as a color image.

Fig. 2.— Diagnostic diagrams, applied to the four brightest galaxies of CG1720-67.8. Squares, diamonds, triangles and crosses represent emission-line ratios (corrected for the underlying stellar component) of objects no. 1, 2, 3, and 4, respectively. Bars denote errors in the line-flux ratios. The solid line in (a), (b), and (c) serves as a dividing line between H II-galaxies (top left) plus low-excitation Starburst-Nucleus Galaxies (SBNG) (bottom left), and Active Galactic Nuclei (AGN) (top right) plus Low Ionization Nuclear Emission-line Regions (LINERs) (bottom right); the dashed line separates H II-galaxies from SBNGs (Coziol et al. 1998), and AGN from LINERs (Coziol 1996).





This figure "fig1.jpg" is available in "jpg" format from:

<http://arxiv.org/ps/astro-ph/9907304v1>